ELSEVIER

Journal of Nuclear Materials 313–316 (2003) 883–887

journal of nuclear materials

www.elsevier.com/locate/jnucmat

Interpretive modeling of simple-as-possible-plasma discharges on DIII-D using the OEDGE code

P.C. Stangeby [a,b,*], J.D. Elder [a], J.A. Boedo [d], B. Bray [b], N.H. Brooks [b], M.E. Fenstermacher [c], M. Groth [c], R.C. Isler [e], L.L. Lao [b], S. Lisgo [a], G.D. Porter [c], D. Reiter [f], D.L. Rudakov [d], J.G. Watkins [g], W.P. West [b], D.G. Whyte [d]

[a] *University of Toronto Institute for Aerospace Studies, 4925 Dufferin St., Toronto, Canada M3H 5T6*
[b] *General Atomics, P.O. Box 85608, San Diego, CA 92186-5608, USA*
[c] *Lawrence Livermore National Laboratory, P.O. Box 808, Livermore, CA 94551, USA*
[d] *University of California, San Diego, 9500 Gilman Drive, La Jolla, CA 90293, USA*
[e] *Oak Ridge National Laboratory, P.O. Box 2008, Oak Ridge, TN 37831, USA*
[f] *University of Duesseldorf, Duesseldorf, Germany and KFA, Jülich, 52425 Germany*
[g] *Sandia National Laboratories, P.O. Box 5800, Albuquerque 87185, Mexico*

Abstract

Recently a number of major, unanticipated effects have been reported in tokamak edge research raising the question of whether we understand the controlling physics of the edge. This report is on the first part – here focused on the outer divertor – of a systematic study of the simplest possible edge plasma – no ELMs, no detachment, etc. – for a set of 10 repeat, highly diagnosed, single-null, divertor discharges in DIII-D. For almost the entire, extensive data set so far evaluated, the matches of experiment and model are so close as to imply that the controlling processes at the outer divertor for these simple plasma conditions have probably been correctly identified and quantitatively characterized in the model. The principal anomaly flagged so far relates to measurements of T_e near the target, potentially pointing to a deficiency in our understanding of sheath physics in the tokamak environment.

PACS: 52.40.Hf
Keywords: OEDGE; DIVIMP; EIRENE; Modeling; Divertor Thompson; Edge spectroscopy

1. Introduction

In the past several years a number of unanticipated major effects have shown up in tokamak edge research, including high tritium retention, strong plasma-wall contact, narrow target power profiles and fast parallel flows. Undoubtedly many parts of our earlier picture remain correct. We need to verify which parts.

This is the motivation for simplest-as-possible plasma (SAPP) studies. The approach:

1. Start with simplest possible conditions, e.g. no ELMs, no detachment.
2. Operate as comprehensive a set of edge diagnostics as possible.
3. Run many repeat shots.
4. Do not put aside any diagnostic unless it is known to be misfunctioning.

* Corresponding author. Address: General Atomics, P.O. Box 85608, San Diego, CA 92186-5608, USA. Tel.: +1-858 455 4518; fax: +1-858 455 2838/4156.
E-mail address: stangeby@fusion.gat.com (P.C. Stangeby).

0022-3115/03/$ - see front matter
PII: S0022-3115(02)01470-8

5. Bring all of the measurements into mutual comparison with an interpretive edge code, such as OEDGE.
6. If most of the data are matched by the code then we may conclude that probably the controlling physics has been correctly identified and quantitatively characterized.
7. Any outstanding discrepancies should be flagged for further investigation as potentially containing important information.

This may provide a solid basis from which to move by steps toward more complicated, more reactor relevant plasmas – as well as a good starting point for sorting out the new edge effects.

A set of 10 identical, low density, $\bar{n}_e \sim 2 \times 10^{19}$ m^{-3}, attached, L-mode, $P_{in}^{total} \sim 1$ MW lower single-null divertor shots on DIII-D has been chosen as SAPP candidate. This report is on the first part of this study – the plasma at the outer target, where the edge diagnostics are particularly comprehensive on DIII-D. Space restrictions, in fact, limit this first report to a sub-set of the outer target data.

2. Diagnostics and interpretive code

The edge diagnostic set on DIII-D is perhaps the most complete of any magnetic confinement device, uniquely including a divertor Thomson scattering, DTS, diagnostic [6] which, with magnetic sweeping of the divertor X-point, provides 2-D measurements of n_e and T_e throughout the divertor. Other diagnostics reported on here: (a) intensity-calibrated filterscope (FS) and multi-chord divertor spectrometry (MDS) systems provided line-of-sight measurements of the intensities of hydrogenic and impurity line emissions across the target; MDS also provided measurements of line widths (temperatures); (b) an extensive target Langmuir probe system provided measurements of I_{sat}^{+} and T_e across the targets. These diagnostics are shown in Fig. 1.

The experimental data are brought into mutual comparison using an iteratively coupled code, OEDGE ('onion-skin modeling + EIRENE + DIVIMP for edge analysis'). EIRENE is a neutral hydrogen Monte Carlo code [1]. DIVIMP is an impurity neutral and ion Monte Carlo code [2]. The Monte Carlo codes require a 'plasma background' into which to launch particles. The onion-skin modeling, OSM, code [3,4] can provide such a background by solving the 1-D, along-**B**, plasma (fluid) conservation equations using across-**B** boundary conditions from experiment, e.g. I_{sat}^{+} and T_e across divertor targets from Langmuir probes [5], to produce a 2-D solution for the edge plasma (toroidal symmetry assumed). The neutral hydrogen-related and impurity-related terms in the OSM's conservation equations are available iteratively as output from the Monte Carlo codes. OSM analysis is insensitive to cross-field transport assumptions, e.g. as to whether it is diffusive or convective; also, transport coefficients such as $D_{\perp}^{SOL}$ and $\chi_{\perp}^{SOL}$ are not required as input in OSM, but instead can be extracted from OSM analysis.

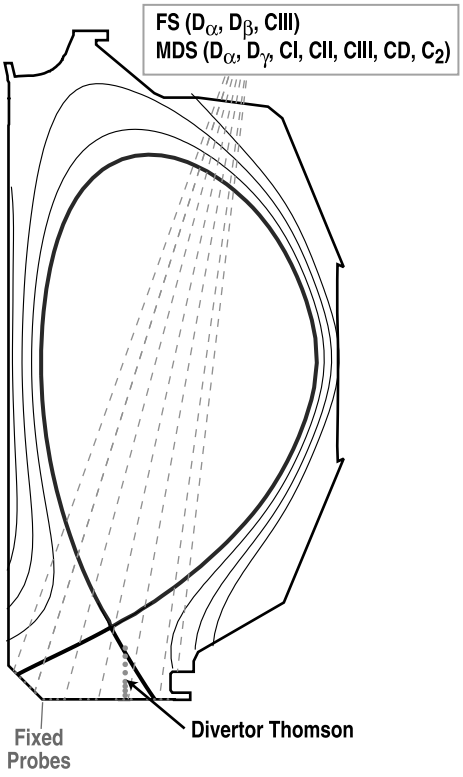

Fig. 1. The DIII-D edge diagnostics used here.

3. Results

The location of the outer strike point was swept during the flattop parts of the shots from $R = 1.62$ to 1.35 m at a constant rate of 10 cm/s. Fig. 2 shows the DTS $T_e(t)$ for different Thomson measuring locations with the times indicated when the separatrix crossed each location. The Thomson laser fired at the same time every 50 ms during each shot. Since the shots were identical, it was possible to significantly improve the statistics of the Thomson analysis by combining the raw data (counts registered by the polychrometers at different wavelengths), greatly reducing the number of rejected data points as well as the scatter. Fig. 2 shows that T_e at each location plunges sharply when the location crosses the separatrix from common to private flux side – generally to within <1 cm. This constitutes an important test of the validity of the EFIT [7] reconstruction of the

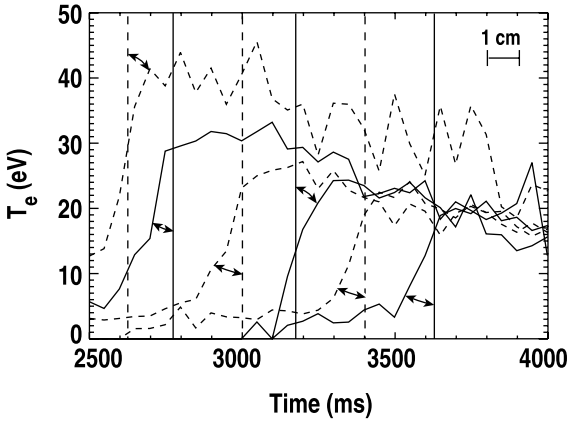

Fig. 2. Divertor Thomson (DTS) $T_e(t)$ profiles for different measuring locations (the maximum T_e increase with height above floor). Verticals indicate separatrix crossing. Combined DTS data for 10 shots.

magnetic equilibrium. The entire undertaking here is dependant on the reliability of the computational grid, Fig. 3, generated from the EFIT equilibrium, since that is required for making mutual comparisons of the various data.

Fig. 4 shows the profiles of T_e and I_{sat}^+ measured across the outer target using the built-in Langmuir probes, as a function of the normalized magnetic flux coordinate ψ_n ($\psi_n = 1$ at the separatrix; $\psi_n > (<)1$ on the common (private) flux side), combining data from six probes for each shot and for all 10 shots. The divertor plasma was found to be constant while being

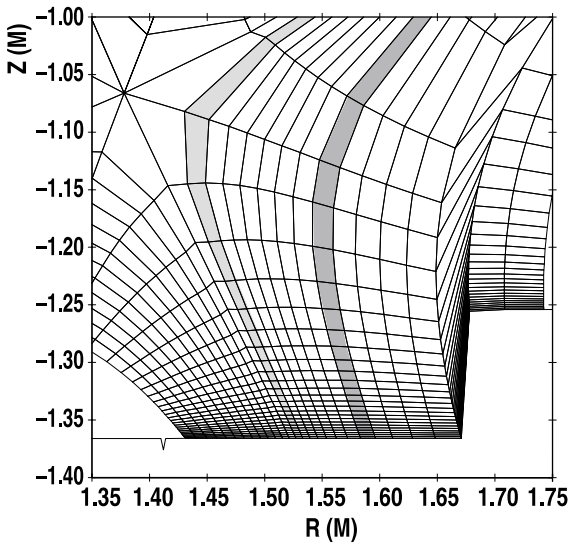

Fig. 3. Computational grid showing poloidal flux surfaces – the 'onion-skin rings'.

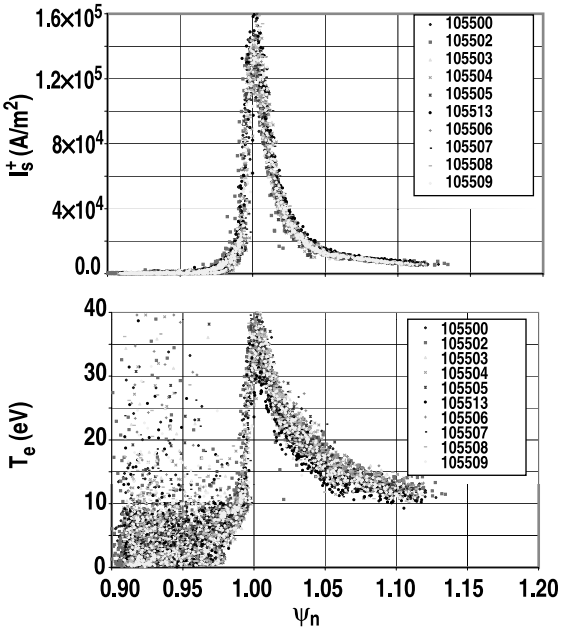

Fig. 4. Langmuir probe outer target profiles of T_e and I_{sat}^+.

swept as evidenced by the different probes, which sample the T and I_{sat}^+ profiles at different times but give indistinguishable profiles. From the trend in Fig. 2 it is seen that the Thomson data extrapolates to a peak target value of about 20 eV, lower than the probe value, about 35 eV. The quantity and quality of both the Thomson and probe data are exceptional – perhaps even uniquely so in tokamak studies – and therefore this discrepancy, which exceeds the scatter and known errors, and is as yet unexplained, has to be flagged as one of potential importance, possibly pointing to a deficiency in our understanding of sheath physics in the tokamak environment, possibly related to non-Maxwellian electrons.

Usually OSM employs target probe T_e and I_{sat}^+ as boundary conditions. Here we use the extrapolated DTS T_e and the probe I_{sat}^+ as boundary conditions, although for the particular measurements reported on here, there is not great sensitivity to values of T_e in this range. Other quantities, to be reported on later, specifically heat flux to the target, are more sensitive to temperature and will, it is hoped, help elucidate this matter.

Fig. 3 shows the poloidal flux surfaces, i.e. the 'onion-rings'. Fig. 5 shows comparisons of OEDGE output with the DTS data for eight outer SOL rings identified by their ψ_n-number. s_{pol} is poloidal distance along **B** from the target. Fig. 6 shows code comparisons with the absolutely calibrated FS and MDS outer target profiles of D_α, D_β, D_γ, CI, CII and CIII. The results in Fig. 6 involved mapping of data from various times in the shot to a single display time, 3500 ms, on the assumption that conditions are the same at the same magnetic coordinates

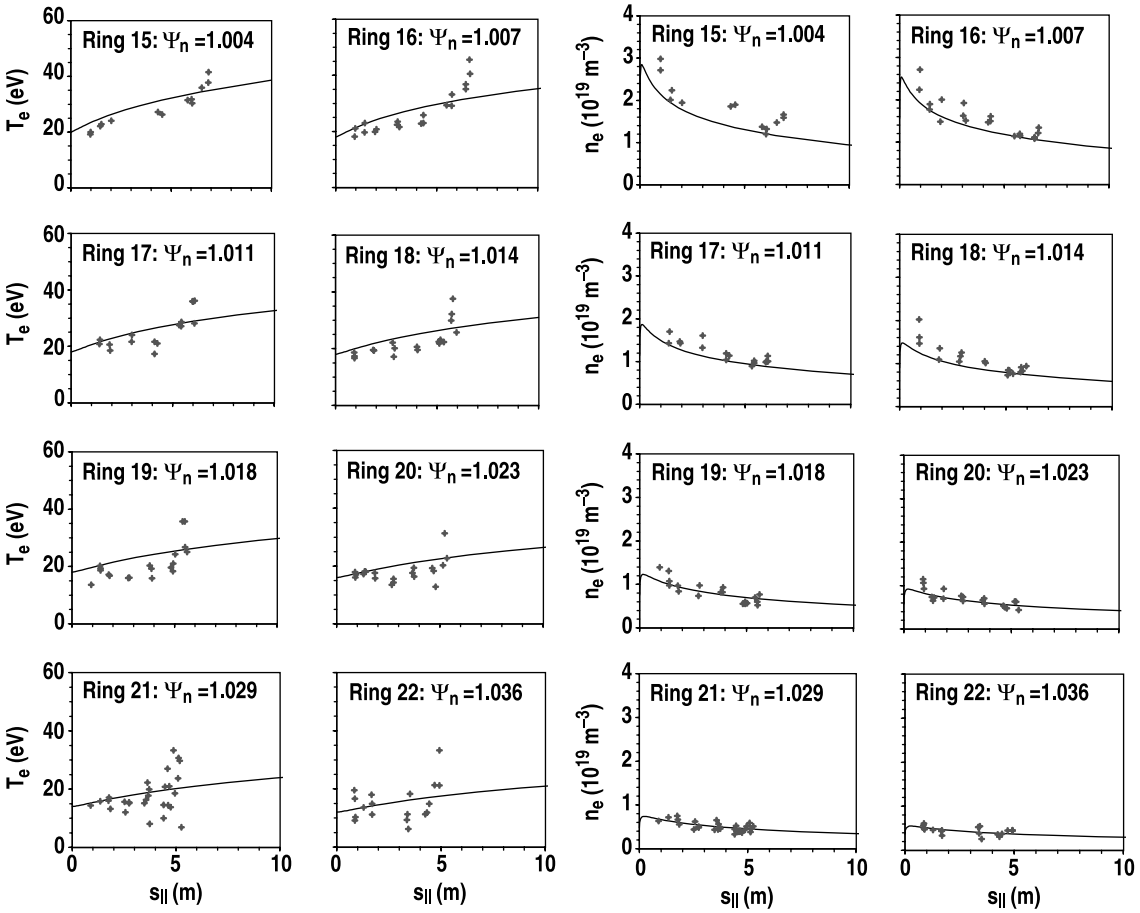

Fig. 5. Profiles of n_e and T_e as functions of distance along **B** ($s_\parallel$) starting at the target for a number of computational 'rings'. Ring No. 15 (22) is the light (dark) shaded flux tube, in Fig. 3 data (points), code (lines). Combined DTS data for 10 shots.

(ψ_n, s_{pol}). The horizontal coordinate in Fig. 6 corresponds to the FS or DTS line-of-sight to the point on the target where the ψ_n-flux line strikes the target. The code results used individual grids and solutions for 41 different times in the sweep. There was almost no detectible CD band radiation at the outer target which was taken to indicate the absence of chemical sputtering. The assumption made in the code, therefore, was that physical sputtering, including self-sputtering, was the sole release mechanism for carbon at the outer target. The normal incidence sputtering yields from [8] were doubled to allow for estimated average incidence angles of ~45°. The effective temperatures from the line widths measured by MDS viewing the outer target are compared with the code output in Table 1. The code value for the C-atom (CI) temperature, 1.25 eV, is the (perhaps surprisingly low) result for a Thompson speed distribution for physically sputtered neutrals, truncated for an assumed D^+ impact energy of 100 eV, a cosine angular distribution, and allowing for the viewing angle of the MDS spectrometer. The truncated Thompson energy distribution given by $f(E) \propto [E/(E+E_B)^3]\{1-[(E+E_B)/\gamma(1-\gamma)E_{impact}]^{1/2}\}$, where $E_B = 7.4$ eV is the C binding energy and $\gamma = 4m_D m_C/(m_D+m_C)^2$, closely matches calculations by the TRSPV1CN Monte Carlo sputtering code results [9]. Chemical sputtering, however, would also be expected to give a CI line temperature of ~1 eV. A more definitive test will be a measurement of the CI line shift, work in progress.

4. Conclusions

The principal conclusion is that these low density SAPP shots on DIII-D appear to constitute the hoped-for starting point: for almost the entire, extensive data set so far evaluated, the matches of experiment and code are so close as to imply that the controlling processes at the outer divertor have probably been correctly identified and quantitatively characterized. The main anomaly

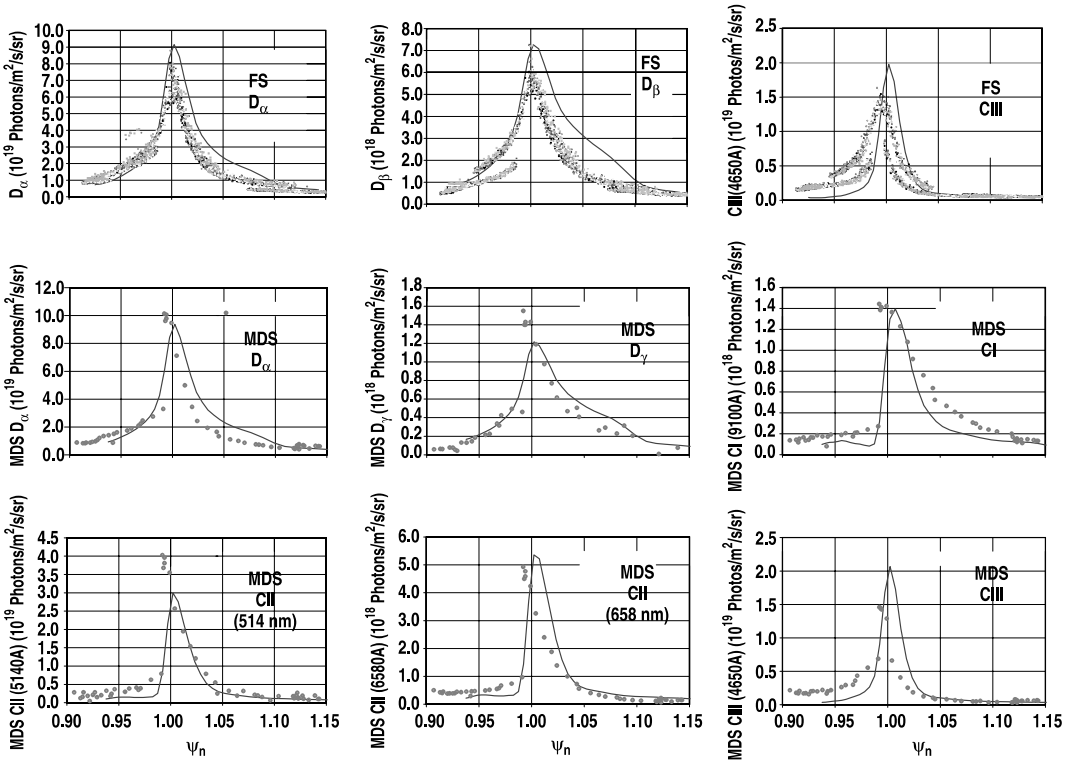

Fig. 6. FS and MDS profiles across the outer target. Data (points). Code (lines).

Table 1
Effective temperatures (eV) from Doppler widths, compared with code values

	Experiment	Code
CI (910 nm)	~0.95	1.25
CII (657.9 nm)	6–7	6.9
CIII (465 nm)	10–15	14.5

flagged so far relates to measurements of T_e near the target, potentially pointing to a deficiency in our understanding of sheath physics in the tokamak environment. Continuing studies including target heat flux measurements using (i) ir, (ii) thermocouple power bolometry will shed light on this critical matter, it is hoped. Other studies, also in progress, will cover the inner target, private flux zone and main chamber of this low density SAPP set. Similar, but higher density sets will then be assessed.

Acknowledgements

Work supported by US Department of Energy under Contracts W-7405-ENG-48, DE-AC04-94AL85000, DE-AC03-99ER54463, and Grant DE-FG03-95ER54294, and by the Natural Sciences and Engineering Research Council of Canada.

References

[1] D. Reiter, J. Nucl. Mater. 196–198 (1992) 80.
[2] P.C. Stangeby, J.D. Elder, Nucl. Fusion 35 (1995) 1391.
[3] P.C. Stangeby, J.D. Elder, W. Fundamenski, et al., J. Nucl. Mater. 241–243 (1997) 358.
[4] W. Fundamenski, P.C. Stangeby, J.D. Elder, J. Nucl. Mater. 266–269 (1999) 1045.
[5] J.G. Watkins, R.A. Moyer, J.W. Cuthbertson, et al., J. Nucl. Mater. 241–243 (1997) 645.
[6] T.N. Carlstrom et al., Rev. Sci. Instrum. 63 (1992) 4901, 66 (1995) 493.
[7] L.L. Lao et al., Nucl. Fusion 30 (1990) 1035.
[8] W. Eckstein, C. Garcia Rosales, J. Roth, W. Ottenberger, Sputtering Data, IPP 9/82, Max-Planck Institut für Plasmaphysik, 1993.
[9] W. Eckstein, V. Philipps, in: W.O. Hofer, J. Roth (Eds.), Fig. 9 in 'Physical Processes of the Interaction of Fusion Plasmas with Solids', Academic Press, New York, 1996.